Acta Crystallographica Section F
Structural Biology and Crystallization Communications
ISSN 1744-3091

Human $tRNA^{Gly}$ acceptor-stem microhelix: crystallization and preliminary X-ray diffraction analysis at 1.2 Å resolution

Charlotte Förster,[a] Karol Szkaradkiewicz,[a] Markus Perbandt,[b] Arnd B. E. Brauer,[a] Tordis Borowski,[a] Jens P. Fürste,[a] Christian Betzel[b] and Volker A. Erdmann[a]*

[a]Institute of Chemistry and Biochemistry, Free University Berlin, Thielallee 63, 14195 Berlin, Germany, and [b]Institute of Biochemistry and Molecular Biology, University of Hamburg, c/o DESY, Notkestrasse 85, Building 22a, 22603 Hamburg, Germany

Correspondence e-mail: erdmann@chemie.fu-berlin.de

Received 25 July 2007
Accepted 23 August 2007

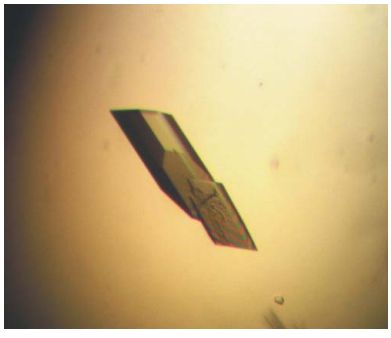

The major dissimilarities between the eukaryotic/archaebacterial-type and eubacterial-type glycyl-tRNA synthetase systems (GlyRS; class II aminoacyl-tRNA synthetases) represent an intriguing example of evolutionarily divergent solutions to similar biological functions. The differences in the identity elements of the respective $tRNA^{Gly}$ systems are located within the acceptor stem and include the discriminator base U73. In the present work, the human $tRNA^{Gly}$ acceptor-stem microhelix was crystallized in an attempt to analyze the structural features that govern the correct recognition of $tRNA^{Gly}$ by the eukaryotic/archaebacterial-type glycyl-tRNA synthetase. The crystals of the human $tRNA^{Gly}$ acceptor-stem helix belong to the monoclinic space group $C2$, with unit-cell parameters $a = 37.12$, $b = 37.49$, $c = 30.38$ Å, $\alpha = \gamma = 90$, $\beta = 113.02^{\circ}$, and contain one molecule per asymmetric unit. A high-resolution data set was acquired using synchrotron radiation and the data were processed to 1.2 Å resolution.

1. Introduction

The apparent simplicity of the amino acid glycine is accompanied by an exceptionally large sequence divergence between the eukaryotic/archaebacterial-type and eubacterial-type GlyRS systems (Shiba, 2005). A detailed analysis of this special system should therefore be particularly instructive in order to understand the underlying structure–function relationship and evolutionary aspects. In the present work, we focus on the human $tRNA^{Gly}$ system in order to complement our recent study on the corresponding *Escherichia coli* system (Förster *et al.*, 2007); in combination, these two studies cover both types of GlyRS system.

The activity of both types of GlyRS is restricted to their corresponding $tRNAs^{Gly}$ (Shiba *et al.*, 1994). This restraint is ensured by the identity elements of the specific $tRNAs^{Gly}$. In the GlyRS system, as in other class II aminoacyl-tRNA synthetase systems (Eriani *et al.*, 1990), the tRNA identity elements assuring the correct aminoacylation of tRNAs with the cognate amino acid consist of only a few simple motifs which are mostly located in the tRNA acceptor stem and often include the discriminator base at position 73.

The eubacterial GlyRS system has been intensively investigated and *E. coli* GlyRS has been shown to be a tetrameric protein consisting of an $\alpha_2\beta_2$ structure (Ostrem & Berg, 1974; Webster *et al.*, 1983). Both the α- and β-subunits contribute to the enzymatic activity of *E. coli* GlyRS (Ostrem & Berg, 1974). The tRNA recognition and binding is governed by the β-subunit (Nagel *et al.*, 1984), whereas the α-subunit is responsible for ATP and glycine binding (Toth & Schimmel, 1990). Eubacterial tRNA identity elements are located in the acceptor stem and include the discriminator base at position 73, which strictly has to be a uracil residue. In the particular case of *E. coli*, the $tRNA^{Gly}$ identity determinants consist of a conserved base pair C2–G71 and the U73 discriminator base (McClain *et al.*, 1991).

The eukaryotic GlyRS system has also been thoroughly studied and a number of different eukaryotic GlyRS sequences have been determined, including those of baker's yeast (Kern *et al.*, 1981), the silkworm *Bombyx mori* (Nada *et al.*, 1993) and human (Shiba *et al.*, 1994). In contrast to the eubacterial-type GlyRSs, eukaryotic enzymes possess an α_2 structure. In addition to the differing quar-

ternary structure of the eukaryotic/archaebacterial-type and eubacterial-type GlyRS, there is a strong sequence divergence of motifs 1–3, which are usually highly conserved among the class II aminoacyl-tRNA synthetases (Eriani *et al.*, 1990; Shiba, 2005). The sequence determinants of the $tRNA^{Gly}$ identity also differ between eukaryotic/archaebacterial-type and eubacterial-type GlyRS systems. The major diversity concerns the discriminator base at position 73, which has to be an adenine residue in eukaryotes, in contrast to a uracil in eubacteria. Structural investigation of the $tRNA^{Gly}$ aminoacyl-stem identity elements contributes to a better understanding of the diversity of the GlyRS system. For example, the crystal structure of the *Thermus thermophilus* GlyRS was analyzed to 2.75 Å resolution (Logan *et al.*, 1995) and revealed a mixture of features of both the eukaryotic/archaebacterial and the eubacterial enzymes. Surprisingly, the architecture of this protein resembles the subunit arrangement of the eukaryotic/archaebacterial-type enzymes, while its aminoacylation activity relies on the 'conventional' eubacterial $tRNA^{Gly}$ identity elements.

We have focused on comparing the high-resolution X-ray structures of $tRNA^{Gly}$ acceptor-stem helices from different organisms. Here, we report the crystallization of the human $tRNA^{Gly}$ acceptor-stem microhelix and its preliminary X-ray diffraction analysis at atomic resolution. This study contributes to the understanding of the structural elements governing the tRNA identity in general (Mueller, Muller *et al.*, 1999; Mueller, Schübel *et al.*, 1999; Ramos & Varani, 1997; Seetharaman *et al.*, 2003, Förster *et al.*, 1999, 2006) and to the comparative structural analysis of the $tRNA^{Gly}$ system in particular (Förster *et al.*, 2007).

2. Materials and methods

2.1. Crystallization of the human $tRNA^{Gly}$ microhelix

HPLC-purified RNA oligonucleotides 5′-GCGUUGG-3′ and 5′-CCAACGC-3′ were purchased from CureVac (Tübingen, Germany). Pellets of lyophilized oligonucleotides were dissolved in water and the RNA concentration was determined according to Sproat *et al.* (1995).

The two complementary strands were annealed in water at 0.5 m*M* concentration each to form the $tRNA^{Gly}$ acceptor-stem duplex. The RNA mixture was heated to 363 K for 5 min and slowly cooled to ambient temperature within several hours. The annealed duplex was used for crystallization experiments.

Initial screening trials were performed using two different screening kits from Hampton Research (CA, USA) designed for nucleic acid crystallization. The Natrix Formulation Screen was applied using the sitting-drop vapour-diffusion technique with CrystalQuick Lp plates from Greiner Bio-One (Germany). Crystallization experiments were prepared by mixing 1 µl of the 0.5 m*M* aqueous solution of RNA duplex with 1 µl reservoir solution. Setups were equilibrated against 80 µl reservoir solution at 294 K. As a second screening procedure, the Nucleic Acid Miniscreen was applied using the hanging-drop vapour-diffusion technique and Linbro Plates (ICN Biomedicals Inc., Ohio, USA). Crystallization setups were prepared by mixing 1 µl of the 0.5 m*M* aqueous RNA solution with 1 µl crystallization solution and were equilibrated against 1 ml 35%(*v*/*v*) MPD (2-methyl-2,4-pentanediol) at room temperature. A crystal with approximate dimensions of 0.1 × 0.05 × 0.05 mm appeared after one week with the following crystallization solution: 40 m*M* sodium cacodylate pH 6.0, 12 m*M* spermine.4HCl, 12 m*M* NaCl, 80 m*M* potassium chloride and 10%(*v*/*v*) MPD at 294 K. Crystallization experiments were performed using this condition without any variation, which led to regularly grown crystals with maximum dimensions of 0.3 × 0.1 × 0.1 mm within several days (Fig. 1). These were used for further analysis.

2.2. Acquisition and processing of X-ray diffraction data

All crystals were flash-frozen using liquid nitrogen directly from the crystallization solution prior to X-ray diffraction data collection; owing to the MPD content of the crystallization solution, no additional cryoprotectant was required. X-ray diffraction data were recorded on the DESY X13 consortium beamline in Hamburg (Germany) at a wavelength of 0.8148 Å using a MAR CCD 165 mm detector. A high-resolution data set was collected from 50 to 1.12 Å

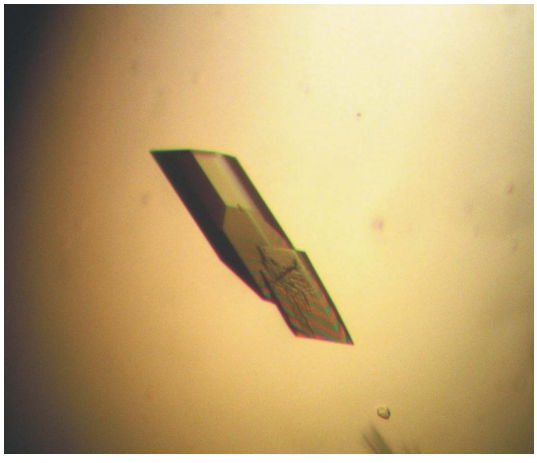

Figure 1
A crystal of the human $tRNA^{Gly}$ acceptor-stem microhelix with approximate dimensions of 0.30 × 0.10 × 0.10 mm.

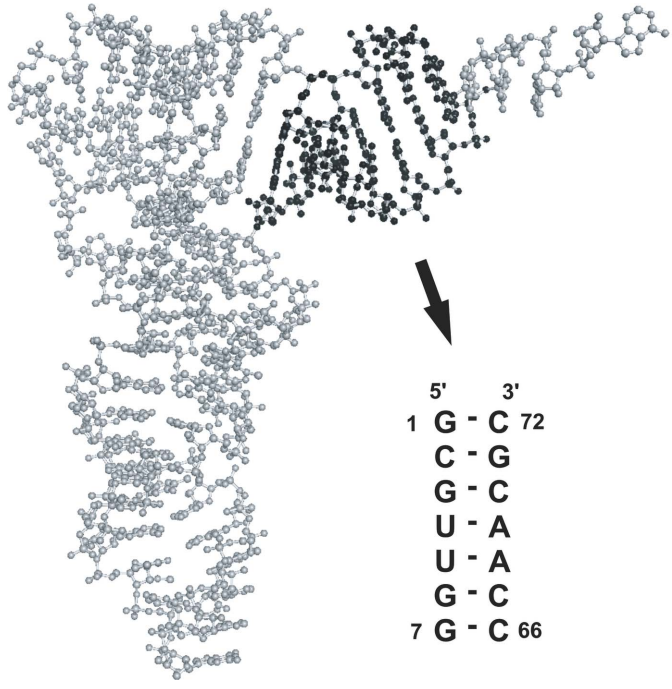

Figure 2
The three-dimensional L-shaped structure of tRNA (designed from $tRNA^{Phe}$; PDB code 1ehz) with the acceptor-stem microhelix segment and the sequence crystallized in this study highlighted in black.

Table 1
Data-collection and processing statistics of the human tRNA^{Gly} acceptor-stem microhelix.

Values in parentheses are for the highest resolution shell.

Beamline	DESY/HASYLAB X13
Wavelength (Å)	0.8148
Space group	*C*2
Unit-cell parameters (Å, °)	a = 37.12, b = 37.49, c = 30.38, β = 113.02
Matthews coefficient V_M (Å^3 Da^{-1})	2.33
RNA duplexes per asymmetric unit	1
Solvent content† (%)	59.4
Measured reflections	83227
Unique reflections	11547
Resolution range (Å)	50.0–1.20 (1.22–1.20)
Completeness (%)	95.3 (93.7)
Multiplicity (%)	7.2 (7.6)
R_{merge}‡ (%)	5.4 (24.9)
$\langle I\rangle/\langle\sigma(I)\rangle$	18.1 (1.46)

† Estimated using the average partial specific volume calculated for RNA by Voss & Gerstein (2005). ‡ $R_{merge} = \sum_{hkl}\sum_i |I_i(hkl) - \langle I(hkl)\rangle|/\sum_{hkl}\sum_i I_i(hkl)$, where $I_i(hkl)$ and $\langle I(hkl)\rangle$ are the observed individual and mean intensities of a reflection with indices hkl, respectively, $\sum_i$ is the sum over the individual measurements of a reflection with indices hkl and $\sum_{hkl}$ is the sum over all reflections.

resolution at 100 K. Data processing and determination of unit-cell parameters and space group were performed using the programs from the *HKL*-2000 suite (Otwinowski & Minor, 1997). The diffraction data were analyzed for merohedral twinning with the Padilla and Yeates algorithm (Padilla & Yeates, 2003) as implemented on the web server http://nihserver.mbi.ucla.edu/pystats.

3. Results and discussion

3.1. Crystallization

In the compilation of tRNA sequences and the sequences of tRNA genes (Sprinzl & Vassilenko, 2005), there are three gene sequences coding for human cytoplasmatic tRNA^{Gly} isoacceptors, with identification codes DG9990, DG9991 and DG9992. The acceptor stems of the DG9990 and DG9991 isoacceptors are identical in sequence, whereas that of the DG9992 isoacceptor differs in one base pair as derived from the gene. The base pair concerned is G3–C70 in DG9992, which is an A3–U70 in the other two human tRNA^{Gly} aminoacyl stems.

The human tRNA^{Gly} microhelix with sequence 5′-$G_1C_2G_3U_4$-$U_5G_6G_7$-3′ and 5′-$C_{66}C_{67}A_{68}A_{69}C_{70}G_{71}C_{72}$-3′ derived from the isoacceptor DG9992 (Fig. 2) could be successfully crystallized, yielding crystals with hexagonal morphology, which were used for X-ray diffraction data collection. A representative crystal with dimensions of 0.3 × 0.1 × 0.1 mm, shown in Fig. 1, appeared after one week.

3.2. Crystallographic data

The human tRNA^{Gly} isoacceptor (Kacar *et al.*, 1992) acceptor-stem microhelix with sequence 5′-$G_1C_2G_3U_4U_5G_6G_7$-3′ and 5′-$C_{66}C_{67}$-$A_{68}A_{69}C_{70}G_{71}C_{72}$-3′ crystallizes in space group *C*2, with unit-cell parameters a = 37.12, b = 37.49, c = 30.38 Å, β = 113.02°. The crystal packing was calculated according to Matthews (1968) and gave a V_M value of 2.33 Å^3 Da^{-1}. This corresponds to one molecule of RNA per asymmetric unit. The solvent content was estimated to be 59.4% as calculated using the RNA parameters of Voss & Gerstein (2005).

Using synchrotron radiation and cryogenic cooling, a high-resolution data set was collected to 1.12 Å at a wavelength of 0.8148 Å. A total of 83 227 reflections corresponding to 11 547 unique reflections were recorded, which reflects a redundancy of 7.2. The crystallographic data were processed within the resolution range 50–1.2 Å with an overall R_{merge} of 5.4% and an overall completeness of 95.3% (Table 1).

As crystal disorder and merohedral twinning may appear within crystals of short RNA helices (Rypniewski *et al.*, 2006; Mueller, Muller *et al.*, 1999; Mueller, Schübel *et al.*, 1999), we examined our X-ray diffraction data for merohedral twinning using the Padilla & Yeates algorithm (Padilla & Yeates, 2003). For the X-ray diffraction data of the human tRNA^{Gly} acceptor-stem microhelix, the results clearly correspond to those of a theoretically untwinned crystal. At present, we have no indication for merohedral twinning for this data set.

Molecular-replacement techniques will be applied in order to solve the high-resolution structure of the human tRNA^{Gly} acceptor-stem microhelix. Various 7-mer RNA crystal helices can serve as models, *e.g.* the tRNA^{Ala} microhelix (PDB code 434d; Mueller, Schübel *et al.*, 1999) or RNA microhelices generated from native tRNA^{Phe} (Shi & Moore, 2000).

The high-resolution X-ray structure of the human tRNA^{Gly} microhelix should provide detailed insights into the distinct local geometric parameters of the RNA and help to visualize the hydration pattern and locations of water molecules surrounding the RNA. In the case of human placenta tRNA^{Gly}, modifications such as 2′-*O*-methylcytidine and 2′-*O*-methyluridine at position 4 or N^2-methylguanosine at position 6 have been described (Gupta *et al.*, 1979, 1980; Sprinzl & Vassilenko, 2005). As our tRNA sequence was derived from the gene sequence (Sprinzl & Vassilenko, 2005), post-translational modification of the human tRNA^{Gly} acceptor stem cannot be excluded. Nevertheless, a comparison between the crystal structure of the *E. coli* tRNA^{Gly} acceptor-stem microhelix (Förster *et al.*, 2007) and the high-resolution X-ray structure of the human tRNA^{Gly} aminoacyl-stem microhelix will contribute to a more detailed understanding of the divergence between eukaryotic/archaebacterial-type and eubacterial glycyl-tRNA synthetase systems at the structural level.

This work was supported within the RiNA network for RNA technologies by the Federal Ministry of Education and Research, the City of Berlin and the European Regional Development Fund. We thank the Fonds der Chemischen Industrie (Verband der Chemischen Industrie e.V.) and the National Foundation for Cancer Research, USA for additional support. We gratefully acknowledge the DESY synchrotron facility, Hamburg for providing beamtime and Svenja Brode and Barbara Schmidt for assistance.

References

Eriani, G., Delarue, M., Poch, O., Gangloff, J. & Moras, D. (1990). *Nature (London)*, **347**, 203–206.
Förster, C., Eickmann, A., Schubert, U., Hollmann, S., Müller, U., Heinemann, U. & Fürste, J. P. (1999). *Acta Cryst.* D**55**, 664–666.
Förster, C., Krauss, N., Brauer, A. B. E., Szkaradkiewicz, K., Brode, S., Hennig, K., Fürste, J. P., Perbandt, M., Betzel, C. & Erdmann, V. A. (2006). *Acta Cryst.* F**62**, 559–561.
Förster, C., Perbandt, M., Brauer, A. B. E., Brode, S., Fürste, J. P., Betzel, C. & Erdmann, V. A. (2007). *Acta Cryst.* F**63**, 46–48.
Gupta, R. C., Roe, B. A. & Randerath, K. (1979). *Nucleic Acids Res.* **7**, 959–970.
Gupta, R. C., Roe, B. A. & Randerath, K. (1980). *Biochemistry*, **19**, 1699–1705.
Kacar, Y., Thomann, H. & Gross, H. (1992). *DNA Cell Biol.* **11**, 781–790.
Kern, D., Giegé, R. & Ebel, J.-P. (1981). *Biochemistry*, **20**, 122–131.
Logan, D. T., Mazauric, M. H., Kern, D. & Moras, D. (1995). *EMBO J.* **14**, 4156–4167.
McClain, W. H., Foss, K., Jenkins, R. A. & Schneider, J. (1991). *Proc. Natl Acad. Sci. USA*, **88**, 6147–6151.

Matthews, B. W. (1968). *J. Mol. Biol.* **33**, 491–497.
Mueller, U., Muller, Y. A., Herbst-Irmer, R., Sprinzl, M. & Heinemann, U. (1999). *Acta Cryst.* D**55**, 1405–1413.
Mueller, U., Schübel, H., Sprinzl, M. & Heinemann, U. (1999). *RNA*, **5**, 670–677.
Nada, S., Chang, P. K. & Dignam, J. D. (1993). *J. Biol. Chem.* **268**, 7660–7667.
Nagel, G. M., Cumberledge, S., Johnson, M. S., Petrella, E. & Weber, B. (1984). *Nucleic Acids Res.* **12**, 4377–4384.
Ostrem, D. L. & Berg, P. (1974). *Biochemistry*, **13**, 1338–1348.
Otwinowski, Z. & Minor, W. (1997). *Methods Enzymol.* **276**, 307–326.
Padilla, J. E. & Yeates, T. O. (2003). *Acta Cryst.* D**59**, 1124–1130.
Ramos, A. & Varani, G. (1997). *Nucleic Acids Res.* **25**, 2083–2090.
Rypniewski, W., Vallazza, M., Perbandt, M., Klussmann, S., DeLucas, L. J., Betzel, C. & Erdmann, V. A. (2006). *Acta Cryst.* D**62**, 659–664.
Seetharaman, M., Williams, C., Cramer, C. J. & Musier-Forsyth, K. (2003). *Nucleic Acids Res.* **31**, 7311–7321.
Shi, H. & Moore, P. B. (2000). *RNA*, **6**, 1091–1105.
Shiba, K. (2005). *The Aminoacyl-tRNA Synthetases*, edited by M. Ibba, C. Francklyn & S. Cusack, pp. 125–134. Georgetown, Texas: Landes Bioscience.
Shiba, K., Schimmel, P., Motegi, H. & Noda, T. (1994). *J. Biol. Chem.* **269**, 30049–30055.
Sprinzl, M. & Vassilenko, K. S. (2005). *Nucleic Acids Res.* **33**, D139–D140.
Sproat, B., Colonna, F., Mullah, B., Tsou, D., Andrus, A., Hampel, A. & Vinayak, R. (1995). *Nucleosides Nucleotides*, **14**, 255–273.
Toth, M. J. & Schimmel, P. (1990). *J. Biol. Chem.* **265**, 1005–1009.
Voss, N. R. & Gerstein, M. (2005). *J. Mol. Biol.* **346**, 477–492.
Webster, T. A., Gibson, B. W., Keng, T., Biemann, K. & Schimmel, P. (1983). *J. Biol. Chem.* **258**, 10637–10641.